Naphthoquinone-based imidazolyl esters as blue-light-sensitive Type I photoinitiators

Fatima Hammoud, Aristea Pavlou, Alexandros Petropoulos, Bernadette Graff, Michael Siskos, Akram Hijazi, Fabrice Morlet-Savary, Frédéric Dumur, Jacques Lalevée

Naphthoquinone-based imidazolyl esters as blue-light-sensitive Type I photoinitiators

Fatima Hammoud[1,2,3], Aristea Pavlou[4], Alex Petropoulos[4], Bernadette Graff[1,2], Michael G. Siskos[4], Akram Hijazi[3], Fabrice Morlet-Savary[1,2], Frédéric Dumur[5*] and Jacques Lalevée[1,2*]

[1] Université de Haute-Alsace, CNRS, IS2M UMR7361, F-68100 Mulhouse, France.

[2] Université de Strasbourg, France.

[3] EDST, Université Libanaise, Campus Hariri, Hadath, Beyrouth, Liban.

[4] Department of Chemistry, Section of Organic Chemistry and Biochemistry, University of Ioannina, Ioannina, 45110, Greece.

[5] Aix Marseille Univ, CNRS, ICR UMR 7273, F-13397 Marseille, France.

Corresponding authors: Frederic.dumur@univ-amu.fr; jacques.lalevee@uha.fr

Abstract:

In this work, a series of Type I photoinitiators (PIs) based on the naphthoquinone scaffold were designed and synthesized for the first time, in order to induce photopolymerization under visible light. As a result, these PIs exhibit excellent photoinitiation abilities in the presence of acrylates monomers upon LED@405 or @455 nm irradiation. Interestingly, some compounds have better photoinitiation performance than the benchmark Type I phosphine-oxide i.e. diphenyl(2,4,6-trimethylbenzoyl)phosphine oxide (TPO) upon exposure to LED@455 nm. Chemical mechanisms supporting the photopolymerization process were investigated through different techniques as well as theoretical calculations. In addition, the new proposed structures were also investigated in two-component photoinitiating systems and exhibited a higher efficiency in free radical photopolymerization. Finally, direct laser write approach is successfully used to fabricate 3D objects.

Keywords: Naphthoquinone-esters, photoinitiators, visible light, 3D objects.

1. Introduction

The process of light-induced polymerization is a field that has attracted a lot of interest in the past few years due to its several environmental benefits, including low energy consumption, low or no volatile organic emissions and high efficiency. [1-3] Consequently, this technology is now extensively used for a large number of industrial applications such as 3D printing, adhesives, coatings, and dentistry. [4-6] Indeed, photoinitiators (PIs) are one of the main component for the initiation of the photopolymerization reaction since the nature of the PI (i.e. its light absorption properties) determines the types of light sources that will be used. They can work as cleavable (Type I PIs) or uncleavable (Type II PIs based on PI/hydrogen or electron donor couple) compounds. [7-9] However, Type II PIs can be easily influenced by the solubility, the electron transfer efficiency or the resin viscosity which can negatively affect the efficacy of the different bimolecular interactions. [10] Conversely, Type I PIs generate reactive radicals by a direct homolytic bond cleavage without any hydrogen donors (co-initiators), which is beneficial in overcoming the drawbacks of Type II PIs. [10-12]

Although the majority of the Type I PIs were sensitive in the UV range, a few PIs such as amino-acteophenones (e.g. Irgacure 369) and phosphine oxides such as diphenyl(2,4,6-trimethylbenzoyl)phosphine oxide (TPO) could be activated by excitation at 405 nm. [13-15] Therefore, for mild conditions, the search for new Type I PIs which are capable of absorbing light at longer wavelengths, is attracting more and more attention these last years.

Light-emitting diodes (LEDs) are a valuable alternative to the traditional irradiation systems due to their low cost, compactness, lightweight and extended lifetime. [16-18] In this context, some Type I PIs have been recently reported.[19-22]

Naphthoquinone derivatives are well established biosourced chromophores in plants, marine organisms or microbes, etc. Interestingly, they can be collected easily without sophisticated synthetic procedures. Recent studies on naphthoquinone derivatives as Type II PIs (multicomponent photoinitiating systems) were reported recently. [23-25]

In the present work, a series of naphthoquinone esters, namely 4,9-dioxo-2-phenyl-4,9-dihydro-1*H*-naphtho[2,3-*d*]imidazol-1-yl esters never synthetized earlier according to the literature, were investigated and proposed as high-performance Type I PIs (See Scheme 1). More precisely, various acid chlorides could be used to form esters with 1-hydroxy-2-phenyl-1*H*-naphtho[2,3-*d*]imidazole-4,9-dione, enabling to

facilely prepare the series of imidazolyl esters. It has to be noticed that this series of imidazolyl esters is unprecedented in the literature and can be compared to the well-known oxime ester PIs that are capable to initiate the cleavage of a N-O bond upon irradiation. Following cleavage, a decarboxylation reaction may also occur, producing initiating aryl or alkyl radicals. It appeared for us to be of interest to investigate this new family of PIs and to examine the possibility for imidazolyl esters to behave as high-performance PIs in comparison with oxime esters or well-established phosphine-oxides (e.g. TPO; Scheme 2). Their photoinitiating ability was investigated upon mild conditions (low intensity and LED@405 nm or 455 nm). Their potential use in photosensitive 3D printing resins is also presented as a proof a high reactivity.

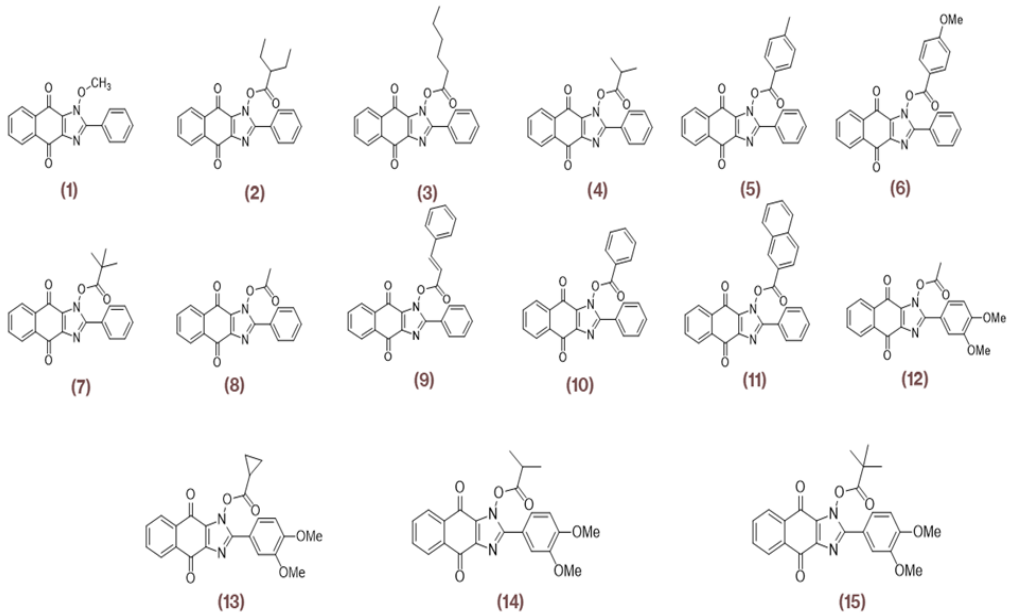

Scheme 1. Chemical structures of the synthesized naphthoquinone-based imidazolyl esters.

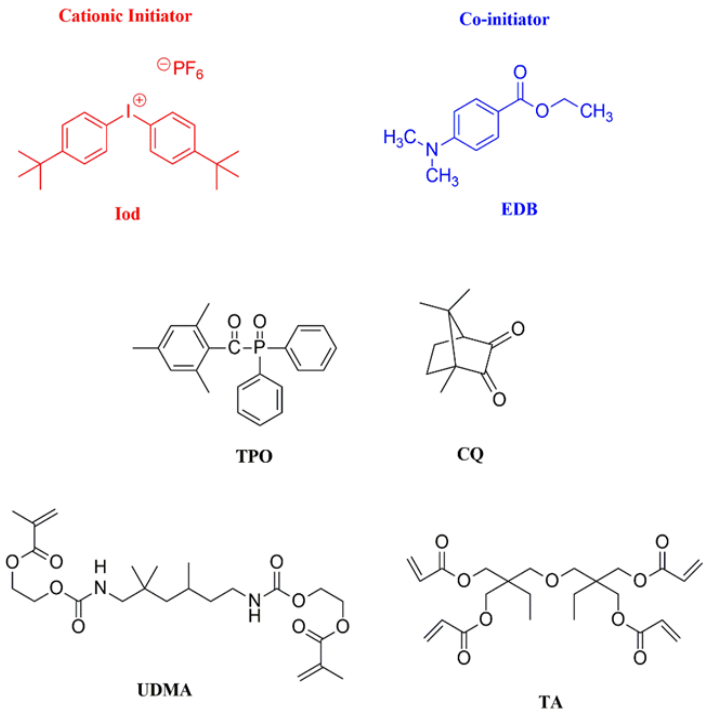

Scheme 2. Chemical structures of the additives and monomers used.

2. Experimental part

2.1. Other Chemicals compounds

Bis-(4-*tert*-butylphenyl)iodonium hexafluorophosphate (Iod), diphenyl(2,4,6-trimethylbenzoyl)phosphine oxide (TPO) and ethyl 4-dimethylaminobenzoate (EDB) were obtained from Lambson Ltd (UK) (Scheme 2). Camphorquinone (CQ, Scheme 2) was obtained from Sigma Aldrich. The monomer di(trimethylolpropane)tetraacrylate (TA) or urethane dimethacrylate (UDMA) were obtained from Allnex (Scheme 2).

2.2. Irradiation Source

Different light emitting diodes (LEDs) are used here as irradiation sources: (i) λ_{em} = 455 nm (labeled as LED@455nm; I_0 = 100 mW cm^{-2}) (ii) λ_{em} = 405 nm (labeled as LED@405nm; I_0 = 110 mW cm^{-2}) and (iii) λ_{em} = 375 nm (labeled as LED@375nm; I_0 = 40 mW cm^{-2}).

2.3. UV-visible absorption and photolysis experiments

The light absorption properties as well as their photolysis ability were investigated by UV-Vis spectroscopy as presented by us in [19] (see more details in supporting information).

2.4. Photopolymerization kinetics (RT-FTIR)

The polymerization kinetics were followed in different experimental conditions (see the Figure captions) by real time FTIR (RT-FTIR) spectroscopy (JASCO FTIR 4600) as presented by us in [26-27] (see more details in supporting information).

2.5. Computational procedure

The Bond Dissociation Energies (BDE), the excited states energy levels and the absorption properties of the different PIs were calculated using the Gaussian 16 suite of programs as presented by us in [19] (see more details in supporting information).

2.6. Fluorescence experiments

The properties of the first singlet excited state (S_1) were probed by steady state fluorescence as well as Time correlated single photon counting (TCSPC) as presented by us in [19]; (see more details in supporting information).

2.7. ESR spin-trapping (ESR-ST) experiments

The free radicals generated were characterized by ESR-ST experiments (an X-band spectrometer ; Bruker EMX-plus) as presented by us in [19] (see more details in supporting information). The free radicals generated were trapped by phenyl-*N*-*tert*-butylnitrone (PBN) based on a procedure described in the literature. [26-27] After the end of the experiment, some ESR simulations were carried out using the PEST WINSIM program.

2.8. Direct Laser Write

To characterize the spatial control of the reaction, direct laser write experiments were performed using a laser diode @405 nm (spot size around 50 μm) (see more details in supporting information). The generated 3D patterns were analyzed using a numerical optical microscope as presented in [19].

3. Results and discussion

3.1. Synthesis of the dyes

All dyes were prepared using 1,4-naphthoquinone (C1) as the starting material (See Scheme 3). By a Michael condensation of benzylamine (C2) and 3,4-

dimethoxybenzylamine (C3), 2-(benzylamino)naphthalene-1,4-dione (C4) and 2-((3,4-dimethoxylbenzyl)amino) naphthalene-1,4-dione (C5) in 92 and 85% yields respectively. By a cyclization reaction previously reported by Lavrikova and coworkers, [28] done in acetic acid and by treatment with a mixture of nitric and sulfuric acids, 1-hydroxy-2-phenyl-1*H*-naphtho[2,3-*d*]imidazole-4,9-dione (C6) and 2-(3,4-dimethoxyphenyl)-1-hydroxy-1*H*-naphtho[2,3-*d*]imidazole-4,9-dione (C7) could be obtained in 67 and 84% yields respectively. 1-Hydroxy-2-phenyl-1*H*-naphtho[2,3-*d*]imidazole-4,9-dione derivatives C6 and C7 were then esterified with different acid chlorides using triethylamine as the base, providing compounds 2-15. Using this strategy, molecules that can be considered as analogues of oxime esters were obtained. For comparison, a molecule bearing a non-cleavable group was prepared. Thus, upon alkylation of C6 with iodomethane in DMF at room temperature and by using potassium *tert*-butoxide as the base, 1-methoxy-2-phenyl-1*H*-naphtho[2,3-*d*]imidazole-4,9-dione (1) could be isolated in pure form in 88% yield.

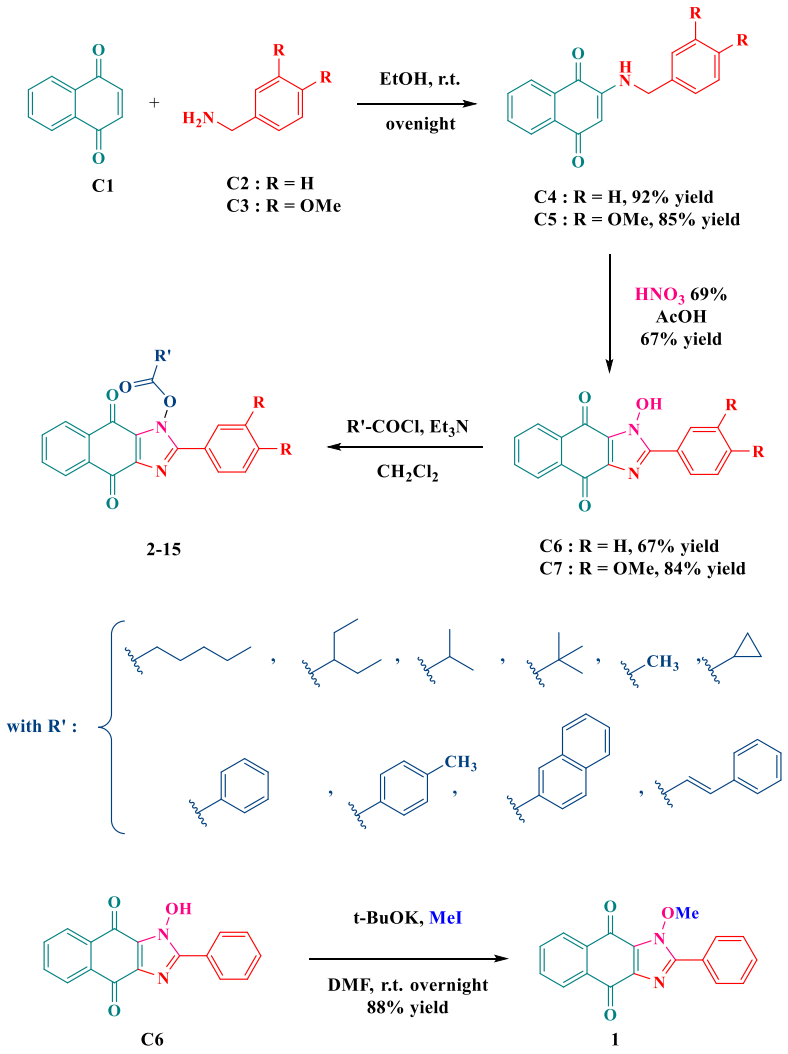

Scheme 3. Synthetic routes to the different dyes.

3.2. UV-Visible Absorption

UV-visible absorption spectra of the studied derivatives (Figure 1) were acquired in acetonitrile (ACN) and the measured properties are gathered in Table 1. Compounds **(1)-(11)** have λ_{max} at around 380 nm, while after the introduction of the two methoxy groups the λ_{max} of the naphthoquinone-esters **(12)-(15)** is blue shifted (Figure 1, Table 1). Besides this blue shift observed for the last series of naphthoquinones, all dyes exhibit a good absorption for the LED light used in this study.

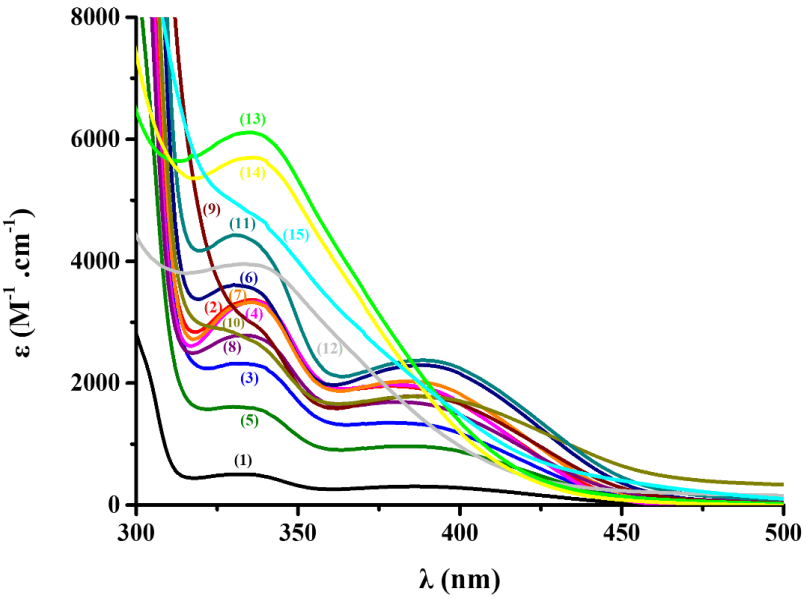

Figure 1. UV-Visible Absorption properties of **1-15** in acetonitrile.

Table 1. Light absorption properties of the investigated compounds: maximum absorption wavelength (λ_{max}), molecular extinction coefficients at λ_{max}, @405 and @455nm.

PIs	λ_{max} (nm)	ε_{max}(M^{-1} cm^{-1})	ε_{405} (M^{-1} cm^{-1})	ε_{455} (M^{-1} cm^{-1})
(1)	330	500	260	30
(2)	380	1950	1500	90
(3)	382	1350	1070	100
(4)	378	1980	1510	40
(5)	383	970	810	100
(6)	388	2300	2010	260
(7)	383	2000	1670	130
(8)	382	1700	1360	170
(9)	387	1800	1550	210
(10)	385	1800	1630	570
(11)	388	2370	2110	360
(12)	333	3960	810	220
(13)	334	6110	1100	120
(14)	336	5700	960	70
(15)	339	4670	1290	360

3.3. Type I Photoinitiator Features

For the benchmark TA monomer, Type I photoinitiation abilities of the investigated compounds (0.5% w) were studied using RT-FTIR in thin (25 μm, in laminate) and thick (1.4 mm under air) samples upon irradiation using different LEDs (405 nm or 455 nm). Typical photopolymerization profiles are shown in Figure 2; the obtained final acrylate function conversions (FCs) are gathered in Table 2.

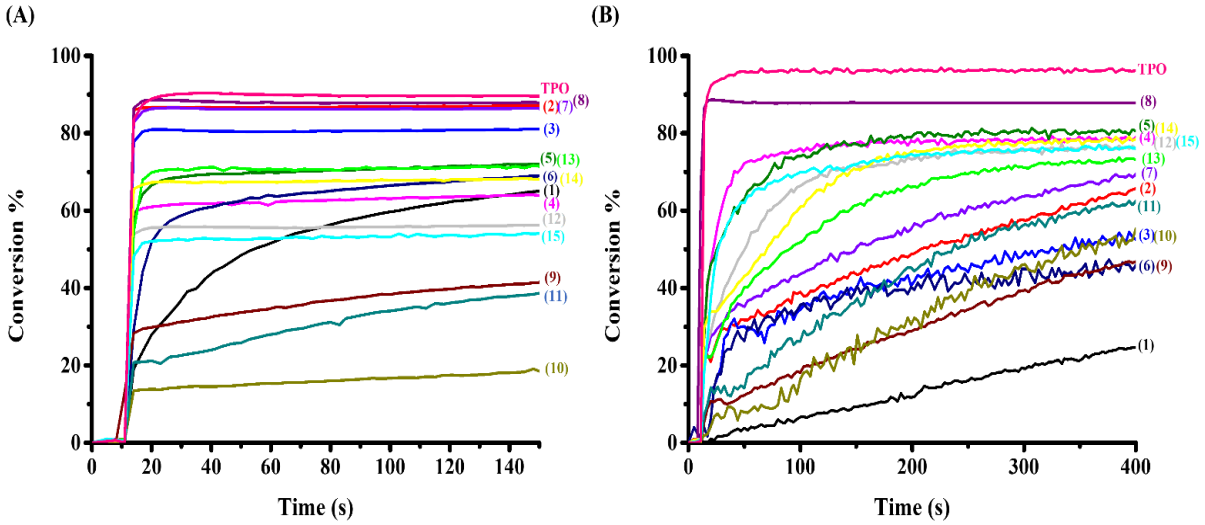

Figure 2. Photopolymerization profiles of TA (acrylate function conversion vs. irradiation time) using one component photoinitiating systems (0.5 % w) in (A) laminate (thickness = 25 μm) and (B) under air (thickness = 1.4 mm); the irradiation with LED (λ = 405 nm) starts at t = 10 s.

Compound **(1)**, which has no ester function, has a very poor photoinitiator behavior compared to the other structures (**2-15**), indicating the role of the ester group to be able to react as a Type I photoinitiator. Compound **(8)** (with a methyl substituent on the carboxyl side) reached the highest FC of 88%, which is also very close to that of the commercial photoinitiator TPO (See Figure 2 and Table 2). Noticeably, compounds with alkyl substituents on the carboxyl side appear to have excellent photoinitiation performance compared to compounds that have aryl substituents (e.g. compounds **(2)**, **(3)**, **(4)**, **(7)**, and **(8)** show fast polymerization rates as well as high final conversions compared to the other compounds - Figure 2(A)). The difference of reactivity (thin vs. thick samples) can be associated with an inner filter effect. Moreover, after introduction of methoxy groups in the structure of the compounds which have alkyl substituents in order to increase their absorption properties, it was clearly noticed that their photoinitiation ability was reduced compared to their analogues without methoxy substituents (see compounds **(12)**, **(13)**, **(14)** and **(15)** vs. compounds **(8)**, **(4)** and **(7)** in

Figure 2). This can clearly show that the photoinitiation ability of the studied compounds is not only associated with their absorption properties, hence it is necessary to consider other factors that can affect the photopolymerization ability, such as the cleavage yields, and the reactivity of the generated radicals. In addition, and in order to show the reactivity of the studied structures at longer wavelengths, photopolymerization experiments were also performed using a LED@455 nm, the results showed a high photoinitiation performance, especially for compounds **(8)**, **(2)**, **(3)**, **(4)** and **(7)** (with alkyl substituents on the carboxyl side). Interestingly, at 455 nm, some compounds are much more efficient than the benchmark TPO (Figure 3, see also Table 2). Again, compound **(8)** showed the highest reactivity, even under LED@455 nm with a FC of 87% for thin sample and 84% for thick sample. Markedly, compound **(8)** exhibited a better performance when compared to commercial references, such as camphorquinone/ethyl dimethylaminobenzoate (CQ/EDB) (0.5%/0.5% w/w) or even Titanocene (Irgacure 784) (0.5% w) (see Figure 3 (C)-(D)), which could demonstrate that compound **(8)** can be considered as a new alternative to benchmarks photoinitiators.

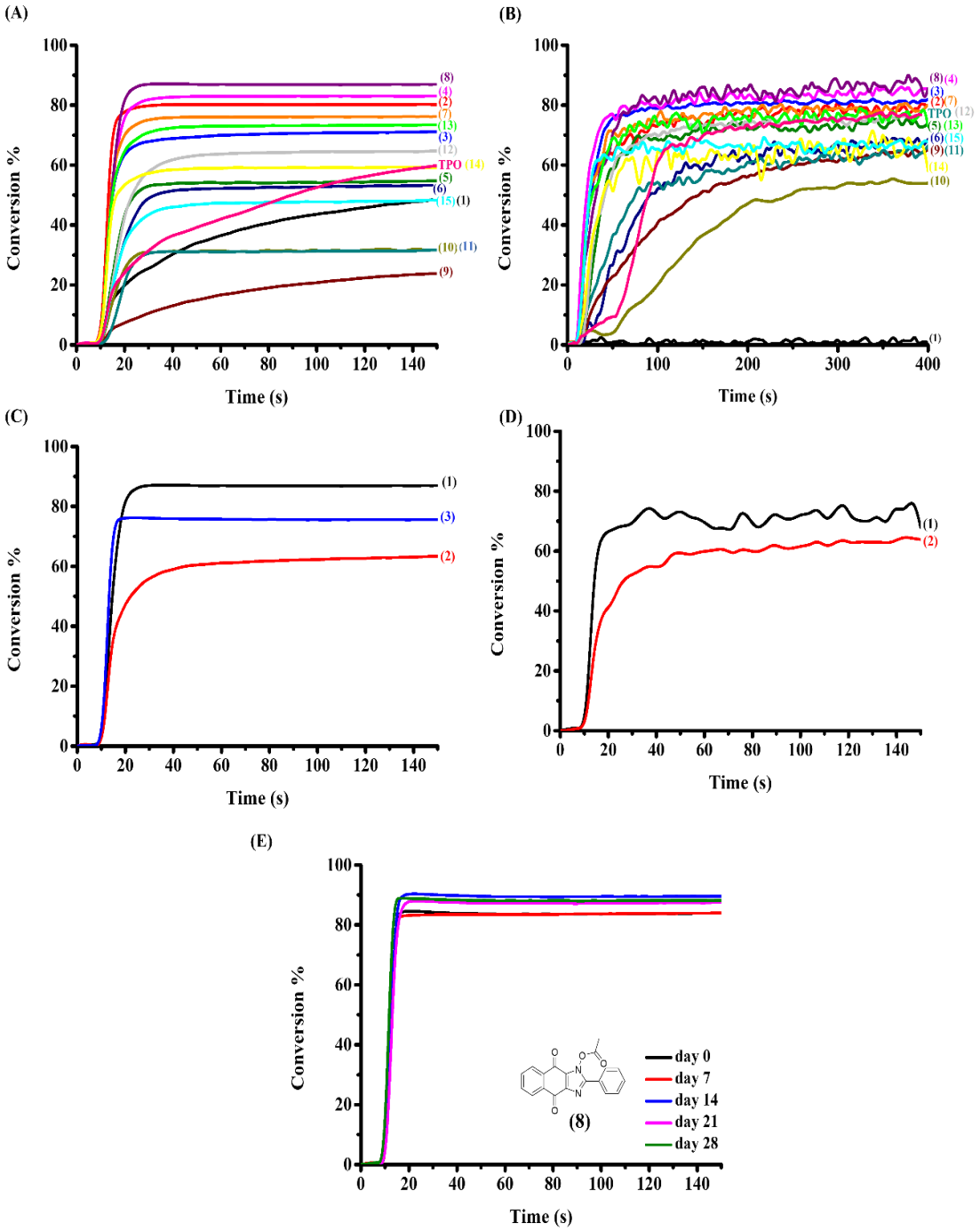

Figure 3. Photopolymerization profiles of TA (acrylate function conversion vs. irradiation time using one component photoinitiating systems (0.5% w) in **(A)** laminate (thickness = 25 μm) and **(B)** under air (thickness = 1.4 mm) upon exposure to a LED light (λ = 455 nm). **(C)** Photopolymerization profiles of TA in laminate (thickness = 25 μm) of (1) compound **(8)** (0,5% w), (2) CQ/EDB (0.5%/0.5% w/w) and (3) Titanocene (0.5% w), **(D)** Photopolymerization profiles of UDMA in laminate (thickness = 25 μm) of (1) compound **(8)** (0.5% w), (2) CQ/EDB (0.5%/0.5% w/w) and **(E)** Photopolymerization profiles of TA using **(8)** (0,5% w) for different storage time in TA monomer. The irradiation starts at t = 10 s.

Compounds **(9)**, **(10)**, **(11)**, **(12)** and **(15)** appear to have the poorest abilities compared to the others. Additionally, compound **(8)** in TA was left for a period of 1

month and its initiation ability was tested weekly. As shown in Figure 3(E), a good storage stability is found without significant decrease of performance.

Table 2. FCs using one component (0.5% w) photoinitiators after 100s of irradiation with LED light (λ = 405 and 455 nm).

PIs	Thin Samples (25 μm) in laminate @405 nm	Thin Samples (25 μm) in laminate @455 nm	Thick Samples (1.4 mm) under air @405 nm	Thick Samples (1.4 mm) under air @455 nm
TPO	90%	61%	95%	77%
(1)	65%	48%	25%	1%
(2)	82%	80%	78%	78%
(3)	68%	71%	84%	81%
(4)	81%	83%	83%	85%
(5)	49%	55%	78%	74%
(6)	34%	53%	48%	68%
(7)	79%	76%	86%	80%
(8)	88%	87%	88%	84%
(9)	42%	24%	48%	65%
(10)	18%	32%	54%	54%
(11)	39%	32%	63%	66%
(12)	56%	65%	76%	78%
(13)	71%	73%	74%	78%
(14)	68%	59%	78%	61%
(15)	54%	48%	76%	67%

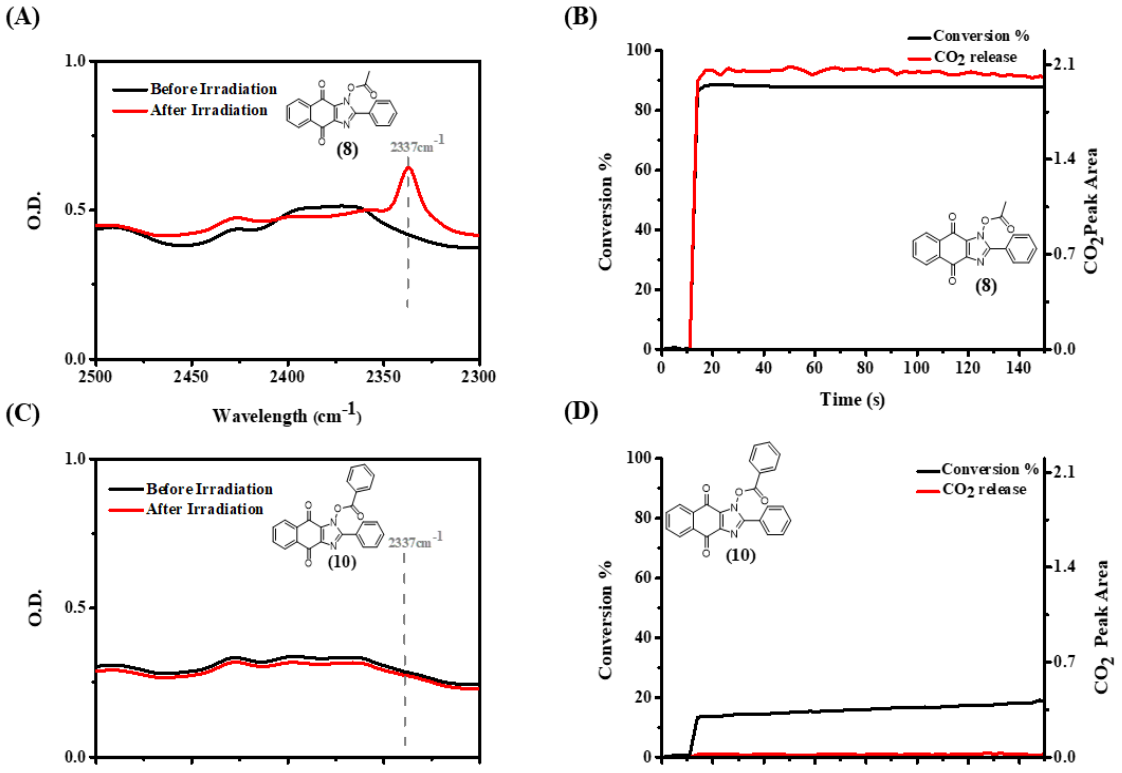

Figure 4. (A) Detection of CO_2 released during photopolymerization using **(8)**, **(B)** Decarboxylation-Conversion correlation using **(8)**, **(C)** Detection of CO_2 released during photopolymerization using **(10)** and **(D)** Decarboxylation-Conversion correlation using **(10);** PI (0.5% w) in TA (thin film polymerization @405nm in laminate).

Remarkably, a release of CO_2 was also observed after irradiation of the photoinitiators in the TA monomer clearly indicating a decarboxylation reaction. Specifically, derivatives with alkyl groups, such as compound **(8)**, appeared to have a peak after irradiation at 2337 cm^{-1}, proving the release of CO_2 (Figure 4(A)). However, derivatives containing an aryl group, such as compound **(10)**, did not show CO_2 release as shown in Figure 4 (C). CO_2 release is an important parameter governing the efficiency of the polymerization as it directly governs the polymerization efficiency (See Figures 4(B) and (D) highlight the link between both profiles). Without CO_2 release, a low yield in initiating radicals is expected.

To better understand the mechanism that occurs after the irradiation of the studied compounds, and more particularly to identify the type of the generated radicals, ESR spin trapping experiments have been performed. Remarkably, when compound **(8)** was irradiated in the presence of phenyl-N-*tert*-butylnitrone (PBN) as spin trapping agent, the ESR signal (a_N = 13.50 G, a_H = 1.86 G) could be assigned to the radical adduct acyloxy radical (RC(=O)O$^{\bullet}$)/PBN (Figure 5). This showed that acyloxy radical

are generated by the cleavage of the N-O bond, which in turn undergo further decarboxylation reactions resulting to carbon centered radicals (Scheme 4), in agreement with the CO_2 release detected by FT-IR during the photopolymerization process (Figure 4 (A)).

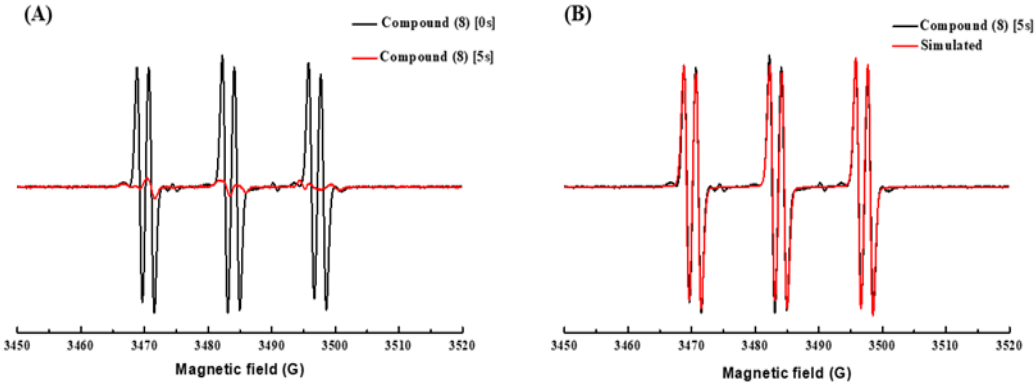

Figure 5. ESR spectra (in presence of PBN and in toluene) recorded for Compound **(8)**: (A) before vs. after irradiation (at t = 0 s and t = 5 s); LED@405 nm. (B) Simulated and experimental spectra observed after irradiation (at t = 30 s).

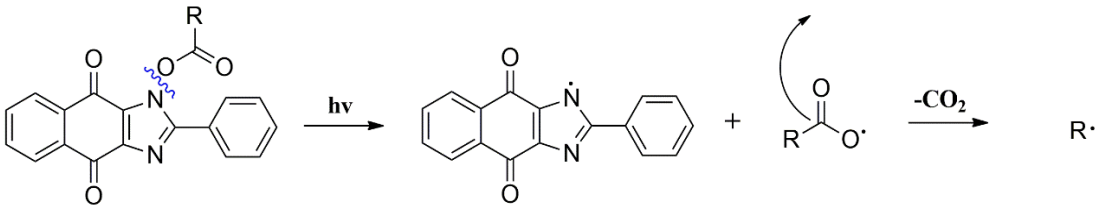

Scheme 4. Proposed photochemical mechanisms for naphthoquinone-based imidazolyl esters.

Photophysical properties of compounds **(8)** and **(10)** (alkyl vs. aryl substituents on the carboxyl side) respectively, are shown in Figure 6. In particular, compound **(8)** (See Figure 6(A)) and all derivatives containing an alkyl substituent have faster photolysis in acetonitrile when irradiated with LED light at 375 nm, compared to compound **(10)** (Figure 6(B)), and even all the derivatives containing aryl substituents, for which no or low photolysis yields was observed. Furthermore, derivatives with methoxy groups, **(12) -(15)**, also show rather rapid photolysis behavior. The above photolysis results are in agreement with the photopolymerization results i.e. high photolysis ability leading to better PI properties.

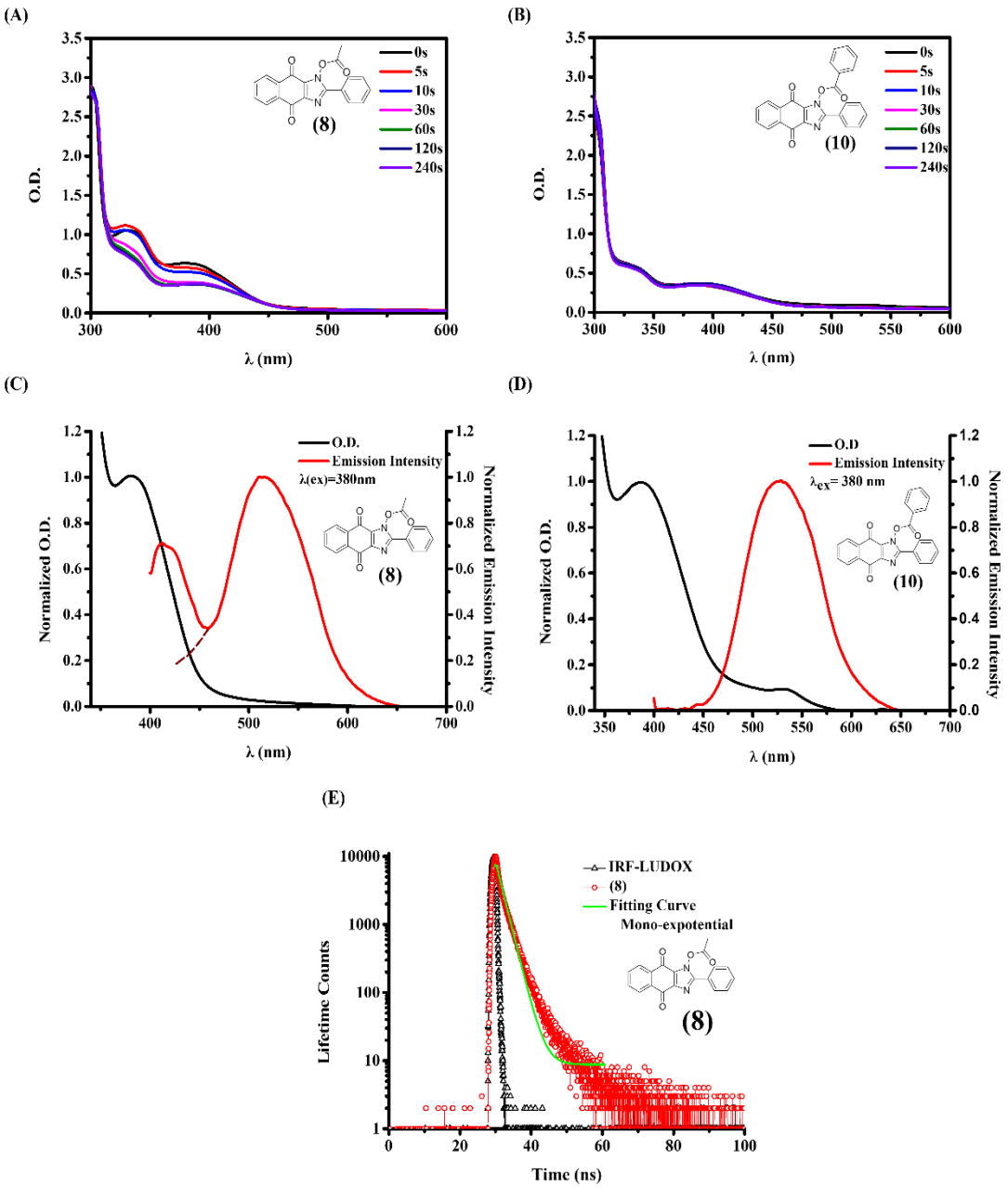

Figure 6. Photolysis of **(A)** compound **(8)** and **(B)** compound **(10)** in acetonitrile using LED light at λ = 375 nm. UV-Visible absorption and emission spectra of **(C)** compound **(8)** and **(D)** compound **(10)** in acetonitrile. **(E)** TCSPC of Compound **(8)** in acetonitrile, λ_{ex} = 367 nm, λ_{em} = 450 nm, and the associated curve fitting.

In Table 3, the corresponding N-O bond dissociation energies (BDE) and excited state properties (singlet and triplet excited states energies) for the studied compounds are given. The N-O cleavage process is energetically favorable from both singlet and triplet excited states from which the dissociation enthalpy of S_1 and T_1 are negative and favorable for compounds **(1)-(11)**. However, more propitious is the

cleavage from the singlet state due to the lower ΔH values. Since compounds (**12)-(15**) did not have any photoluminescence, the singlet state energy could not be evaluated, but they have negative enthalpy values from the triplet state showing that the cleavage is favorable from that energy state. The fluorescence lifetimes of the naphthoquinone-based imidazolyl esters were also measured (Table 3, Figure 6). Derivative without ester function, namely compound **(1),** had the highest lifetime at 3.45 ns, which comes to agreement with its photochemical results i.e. the addition of the ester group provides lower lifetimes suggesting a cleavage from S_1.

Table 3. Parameters characterizing the investigated naphthoquinone-based imidazolyl esters. Parameter calculated by molecular modelling: the bond dissociation energy BDE (N–O), the triplet state energy E_{T1}, the enthalpy ($\Delta H_{cleavageT1}$) for the cleavage process from T_1 ($\Delta H_{cleavageT1}$ = BDE – E_{T1}), the singlet excited state energy E_{S1} (evaluated from the experimental absorption and fluorescence spectra), the enthalpy ($\Delta H_{cleavageS1}$) for the cleavage process from S_1 ($\Delta H_{cleavageS1}$ = BDE - E_{S1}).

PIs	BDE (kcal/mol)	E_{S1} (kcal/mol)	τ_0 (S_1) (ns)	$\Delta H_{cleavageS1}$ (kcal/mol)	E_T (kcal/mol)	$\Delta H_{cleavageT1}$ (kcal/mol)
(1)	41.78	62.3	3.45	-20.51	50.98	-9.2
(2)	35.76	63.5	2.49	-27.74	50.57	-14.81
(3)	36.54	63.8	2.46	-27.26	50.69	-14.15
(4)	34.95	63.5	1.76	-28.55	50.76	-15.81
(5)	34.90	62.2	2.75	-27.3	50.77	-15.87
(6)	34.94	62.6	2.63	-27.66	50.76	-15.82
(7)	35.03	62.8	3.09	-27.77	50.53	-15.50
(8)	36.19	65.13	2.36	-28.94	50.71	-14.52
(9)	34.92	64.3	2.41	-29.38	50.47	-15.55
(10)	34.87	61.8	2.56	-26.93	50.75	-15.88
(11)	34.78	62.6	2.57	-27.82	50.77	-15.99
(12)	32.68	-	-	-	47.12	-14.44
(13)	32.38	-	-	-	47.56	-15.18
(14)	31.41	-	-	-	47.29	-15.88
(15)	31.89	-	-	-	47.82	-15.93

Interesting results were also obtained during the direct laser write experiments at 405 nm under air, in particular with the derivative **(8)** even for very low content (0.1% w) in TA with a short writing time (~ 4s). Figure 7 shows the 3D patterns elaborated with high resolution.

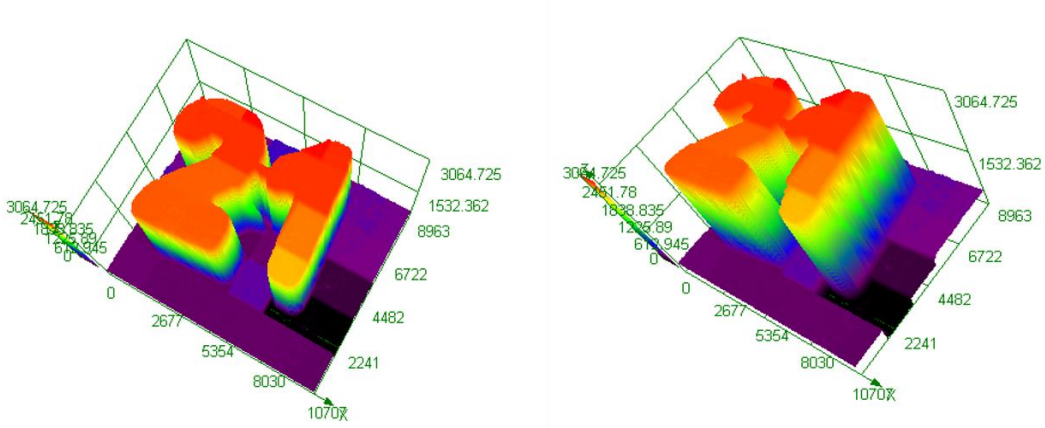

Figure 7. Characterization of the 3D patterns obtained from compound **(8)** (0.1% w) in TA.

3.4. Type II Photoinitiator Features

The photoinitiating ability of OXE/Iod or OXE/EDB (0.1%/1% w/w) was also investigated upon irradiation using a LED@405 nm. The typical polymerization profiles using compound **(13)** are presented in Figure 8; and the final acrylate conversions (FCs) for all the FCs with the other compounds are summarized in Table 4.

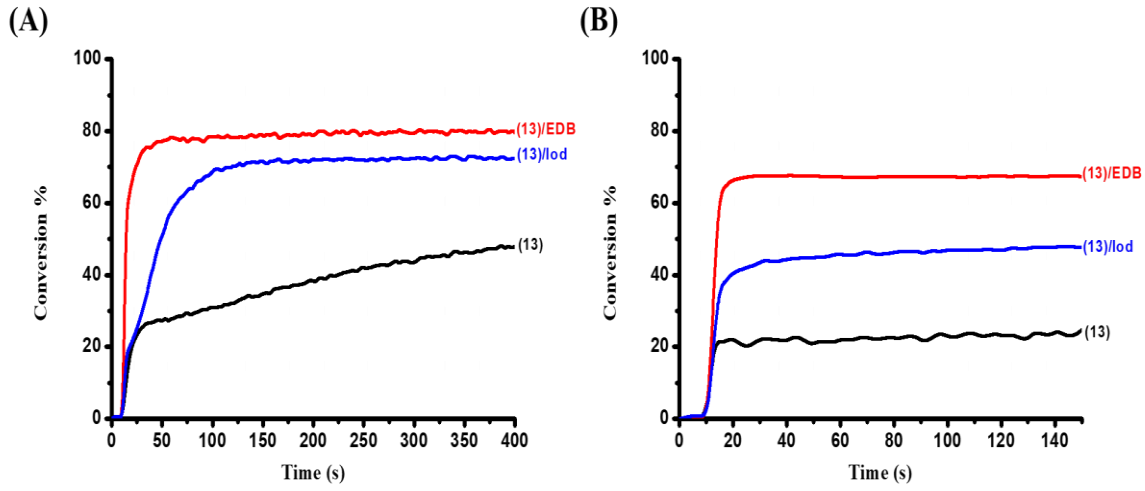

Figure 8. Photopolymerization profiles of TA (acrylate function conversion vs. irradiation time using compound **(13)** alone (0.1% w), compound **(13)**/EDB (0.1%/1% w/w) and compound **(13)**/Iod (0.1%/1% w/w): **(A)** in laminate (thickness = 25 μm) and **(B)** under air using a thickness of 1.4 mm); the irradiation with a LED (λ = 405 nm) starts at t = 10 s.

Table 4. Final Acrylate function conversion using one component (0.1% w) photoinitiator and two-components (0.1%/1% w/w) photoinitiators with Iodonium salt or EDB after 100s of irradiation with LED light (λ = 405 nm).

	Thickness (25 μm) in laminate			**Thickness (1.4 mm) under air**		
	PI	**PI/Iod**	**PI/EDB**	**PI**	**PI/Iod**	**PI/EDB**
(1)	60%	28%	83%	16%	56%	64%
(2)	43%	63%	74%	62%	84%	87%
(3)	43%	48%	53%	69%	84%	85%
(4)	37%	60%	61%	65%	85%	86%
(5)	30%	27%	54%	58%	73%	84%
(6)	48%	47%	67%	52%	70%	85%
(7)	32%	56%	69%	64%	81%	86%
(8)	29%	59%	73%	70%	84%	85%
(9)	44%	38%	66%	47%	63%	88%
(10)	45%	31%	62%	62%	76%	84%
(11)	41%	61%	49%	66%	70%	86%
(12)	39%	52%	55%	37%	46%	81%
(13)	25%	48%	67%	48%	72%	80%
(14)	23%	46%	51%	48%	75%	81%
(15)	62%	46%	6%	42%	57%	78%

When the Iodonium salt was introduced into the light sensitive formulations, most derivatives showed insignificant improvements in their photopolymerization profiles. There was only compound that had a great enhancement in its photopolymerization profile, which was compound **(13)** which had a better performance, reaching a FC of 48%, which is much higher than the 25% that was obtained when compound **(13)** was alone in thin sample. The same effect was also observed in the thick sample where the FC reached 72% compared to 48% when the compound **(13)** was used alone. This fact shows that compound **(13)** is very effective in the photo-oxidation process to initiate a free radical polymerization in combination with Iod (see r3 below).

On the other hand, when EDB was added to the photosensitive formulations, we observed a clear and significant enhancement of the photopolymerization profiles of all compounds on both thin and thick samples. Again, the most remarkable improvement was obtained for compound **(13)** which achieved a final acrylate conversion of 67%,

compared to 25% alone in thin and 48% when combined with Iod. A great enhancement was also seen on the thick sample of Compound **(13)** where the final acrylate conversion reached 80% plus EDB, a result that shows that this compound is also very effective in a photo-reduction process to initiate free radical polymerizations (see r2 below). From the above results, it can easily be understood that these naphthoquinone-based derivatives can work efficiently according to the reactions (r1-r3):

$$PI\ (h\nu) \rightarrow {}^{*}PI \rightarrow R^{\bullet} \qquad (r1)$$

$$^{1}PI + EDB \rightarrow PI^{\bullet -} + EDB^{\bullet +} \rightarrow PI^{\bullet}\text{-}H + EDB^{\bullet}_{(-H)} \qquad (r2)$$

$$^{1}PI + Ar_2I^{+} \rightarrow PI^{\bullet +} + Ar^{\bullet} + ArI \qquad (r3)$$

When the compounds were used as Type I photoinitiators, they could undergo a decarboxylation reaction after the bond cleavage takes place (see r1 below or Scheme 4). This does not seem to be the case when these derivatives are used as Type II photoinitiators with the addition of Iod. As seen in Figure 9 ((A) and (B)), compound **(13)** does not undergo a decarboxylation reaction when Iod is present i.e. we can assume that the excited state is mainly quenched by Iod (r3) than cleaved through (r1) (r1 and r3 being in competition). When the same compound is used in a two-component system with EDB instead of Iod, a decarboxylation reaction takes place, which is in full agreement with the better photopolymerization profile of that derivative plus EDB. This decarboxylation in presence of EDB result is also in agreement with the decarboxylation of the radical anion of oxime-esters ($PI^{\bullet -}$) found in [29].

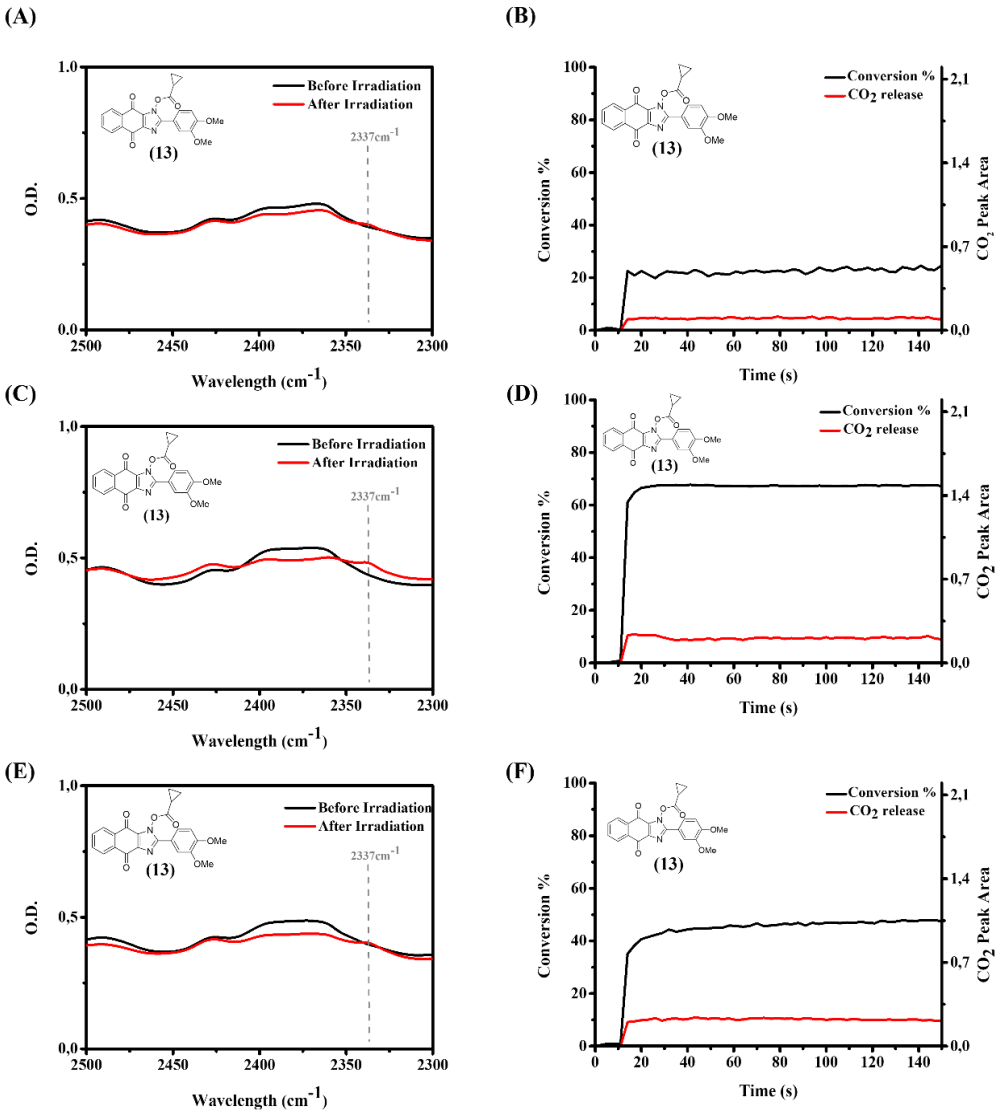

Figure 9. Photopolymrization of TA upon irradiation with a LED@405 nm: **(A)** Detection of CO_2 with **(13)** (0.1% w) system, **(B)** Decarboxylation-Conversion correlation with compound **(13)** (0.1 %w) system, **(C)** Detection of CO_2 with **(13)**/EDB (0.1%/1% w/w) system and **(D)** Decarboxylation-Conversion correlation with **(13)**/EDB (0.1%/1% w/w) system, **(E)** Detection of CO_2 with **(13)**/Iod (0.1%/1% w/w) system, **(F)** Decarboxylation-Conversion correlation with **(13)**/Iod (0.1%/1% w/w) system.

Figure 10 represents the steady state photolysis for **(13)**/Iod or EDB (10^{-2} M) systems in acetonitrile upon irradiation. As observed, there are differences showing that there is an overlap of peaks when adding an additive (Figure 10 (A) vs. (B) and (C)). Furthermore, the addition of EDB to the system leads to a faster photolysis reaction, which is in agreement with the photopolymerization profiles described above. Regarding the rest of the examined type II derivatives, higher polymerization rates were observed for all compounds with alkyl groups in the presence of additives. On the other

hand, the opposite was noted for compounds containing an aryl substituent attached to the ester function.

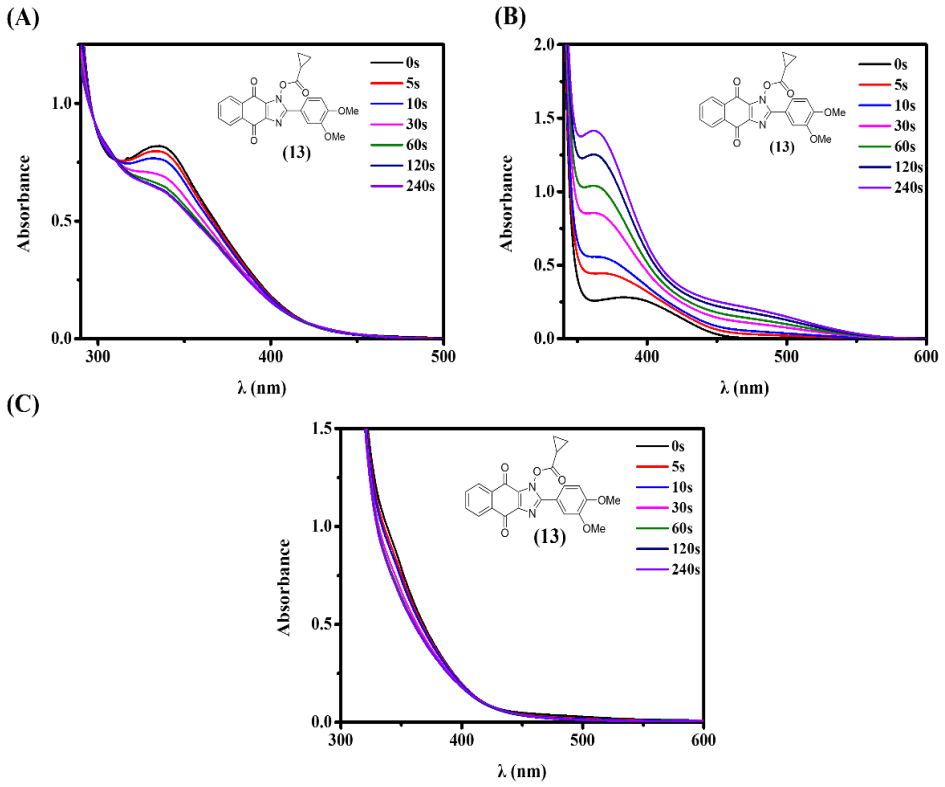

Figure 10. Photolysis of: **(A) (13)** (0.1%w), **(B) (13)**/EDB (10^{-2} M) and **(C) (13)**/Iod (10^{-2} M) in acetonitrile using LED light at λ = 375 nm.

For a better understanding of their interactions with Iod or EDB, fluorescence quenching experiments were carried out in acetonitrile for the different investigated PIs (Figure 11). The concentration of EDB or Iodonium salt was being increased successively and each time a fluorescence spectrum was obtained. The fluorescence quenching was determined from the evolution of the first peak (at ~420 nm) for different contents of EDB or Iod. Indeed, the longest wavelength fluorescence peak was affected (See Figure 11(E)) by the formation of fluorescent photoproducts generated in the photolysis of PI/Iod (or EDB) (See Figure 11(A) and (B)). From the Stern-Volmer equation, the fluorescence quenching yield is calculated:

$$\frac{\Phi_0}{\Phi} = 1+k_{sv}[Q] = 1+k_q \tau_0 [Q] \Rightarrow \Phi_{quenching} = \frac{k_{sv}[Q]}{1+(k_{sv}[Q])}$$

In this latter equation, K_{SV}, k_q , τ_0 and [Q] stand for the Stern-Volmer quenching constant, the bimolecular quenching constant, the unquenched lifetime, the quencher concentration, respectively. [30] All the fluorescence quenching yields are gathered in

Table 5.

Choosing the derivative with the best photoinitiating performance so far, the fluorescence quenching showed that compound **(8)** had one of the highest fluorescence quenching yields when adding iodonium salt but one of the lowest when adding EDB based on the Stern-Volmer equation (See Figures 11(C), (D), (E), (F)). However, compound **(1),** when adding the iodonium salt, had the highest quenching yield, of 97%, but when adding EDB it appeared to be of 39%. Iodonium salt results to higher quenching compared to EDB for derivatives **(1)**, **(8)** and **(11)**. For the other derivatives, however, the opposite phenomenon was observed. Compounds **(3)**, **(4)** and **(9)** appeared to have a blue shift and a hyperchromic effect by the addition of the iodonium salt or EBD and therefore the quenching yield was not calculated.

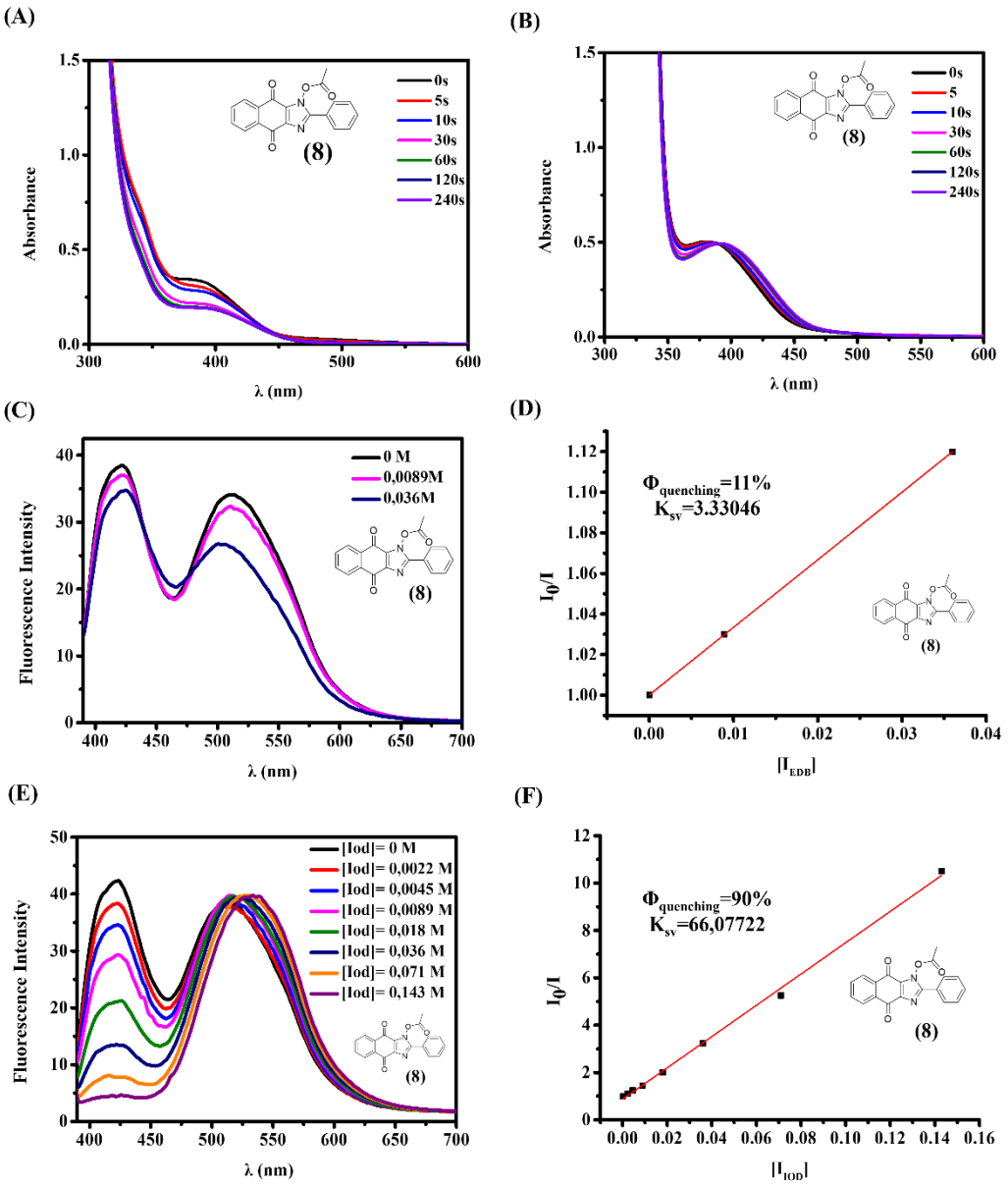

Figure 11. Photolysis of **(A) (8)**/Iod (10^{-2} M) and **(B) (8)**/EDB (10^{-2} M) in acetonitrile using LED light at λ = 375 nm. **(C)** Fluorescence quenching study of compound **(8)** by EDB in acetonitrile and **(D)** representation of the associated Stern-Volmer plot, **(E)** Fluorescence quenching study of compound **(8)** by iodonium salt in acetonitrile and **(F)** associated Stern-Volmer plot for **(E)**.

Table 5. Parameters characterizing the photochemical mechanisms associated with ^{1}PI/Iod or ^{1}PI/EDB interactions.

Compounds	Iod		EDB	
	$\phi_{quenching}$	K_{sv} (M^{-1})	$\phi_{quenching}$	K_{sv}(M^{-1})
(1)	97%	3884	39%	35
(2)	18%	6	43%	20
(5)	23%	2	29%	22
(6)	42%	10	57%	37
(7)	22%	15	44%	42
(8)	90%	66	11%	3
(10)	38%	4	55%	34
(11)	50%	7	43%	41

4. Conclusion

An unprecedented series of naphthoquinone-based imidazolyl esters was designed and successfully synthesized. All the photoinitiators showed interesting photophysical and photochemical properties. These newly synthesized compounds could also provide high photopolymerization conversions as Type I and as Type II photoinitiators when adding a second component into the photoinitiating system, which was either EDB or Iodonium salt. Especially, the naphthoquinone-based derivatives with lower conversions as Type I managed to have higher conversions when acting as Type II. This new family of naphthoquinone-based imidazolyl ester structures show great photoinitiating behavior and more specifically compound **(8)** (with methyl substituent in the carboxyl side) can possibly replace or stand on par with the well-established reference like TPO. Interestingly, these naphthoquinone derivatives have been used for 3D printing experiments. Specific Type I and Type II photoinitiators based on the naphthoquinone scaffold will be presented in forthcoming studies.

Acknowledgements: This research project was supported by The Agence Nationale de la Recherche (ANR) for the NoPerox project (ANR-19-CE07-0042).

5. References

[1] J. P. Fouassier, Photoinitiation, Photopolymerization, and Photocuring: Fundamentals and Applications, Hanser Publishers, New York 1995.

[2] P. Garra, C. Dietlin, F. Morlet-Savary, F. Dumur, D. Gigmes, J.P. Fouassier, J. Lalevée, Photopolymerization processes of thick films and in shadow areas: a review for the access to composites, Polymer Chemistry, 2017, 8.46, 7088-7101.

[3] J. P. Fouassier, J. Lalevée, Photoinitiators: Structures, Reactivity and Applications in Polymerization, Wiley, Weinhein, 2021.

[4] Y. Yagci, S. Jockusch, N. J. Turro, Photoinitiated polymerization: advances, challenges, and opportunities, Macromolecules, 2010, 43, 6245-6260.

[5] F. Karasu, C. Croutxé-Barghon, X. Allonas, D. V. Van, G. J. Leendert, Free radical photopolymerization initiated by UV and LED: Towards UV stabilized, tack free coating, J Polym Sci, Part A: Polym Chem, 2015, 52.24, 3597-607.

[6] F. Hammoud, M. Rahal, J. Egly, F. Morlet-Savary, A. Hijazi, S. Bellemin-Laponnaz, M. Mauro, J. Lalevée, Cubane Cu4I4(phosphine)4 complexes as new co-initiators for free radical photopolymerization: towards aromatic amine-free systems, Polymer Chemistry, 2021, 12, 2848–2859.

[7] J. Lalevée, J. P. Fouassier, Dye Photosensitized Polymerization Reactions: Novel Perspectives, RSC Photochemistry Reports, Ed. A. Albini, E. Fasani, Photochemistry, London, UK, 2015, 215–232.

[8] J. Xu, G. Ma, K. Wang, J. Gu, S. Jiang, J. Nie, Synthesis and photopolymerization kinetics of oxime ester photoinitiators, Journal of Applied Polymer Science, 2012, 123.2, 725-731.

[9] K. Dietliker, T. Jung, J. Benkhoff, H. Kura, A. Matsumoto, H. Oka, D. Hristova, G. Gescheidt, G. Rist, New developments in photoinitiators, Macromolecular Symposia. Weinheim : WILEY-VCH Verlag, 2004. 217.1, 77-98.

[10] S. Liu, B. Graff, P. Xiao, F. Dumur, J. Lalevée, Nitro-Carbazole Based Oxime Esters as Dual Photo/Thermal Initiators for 3D Printing and Composite Preparation, Macromolecular Rapid Communications, 2021, 42.15, 2100207.

[11] F. Hammoud, N. Giacoletto, M. Nechab, B. Graff, A. Hijazi, F. Dumur, J. Lalevée, 5, 12-Dialkyl-5, 12-dihydroindolo [3, 2-a] carbazole-Based Oxime-Esters for LED Photoinitiating Systems and Application on 3D Printing. Macromolecular Materials and Engineering, 2022, 2200082.

[12] P. Hu, W. Qiu, S. Naumov, T. Scherzer, Z. Hu, Q. Chen, W. Knolle, Z. Li, Conjugated bifunctional carbazole-based oxime esters: Efficient and versatile photoinitiators for 3D Printing under one-and two-photon excitation. ChemPhotoChem, 2020, 4.3, 224-232.

[13] A. Kowalska, J. Sokolowski, K. Bociong, The photoinitiators used in resin based dental composite—a review and future perspectives, 2021, Polymers, 13.3, 470.

[14] C. Dietlin, T. T. Trinh, S. Schweizer, B. Graff, F. Morlet-Savary, P. A. Noirot, J. Lalevée, New phosphine oxides as high performance near-UV type I photoinitiators of radical polymerization, Molecules, 2020, 25.7, 1671.

[15] M. A. Tehfe, F. Dumur, B. Graff, F. Morlet-Savary, D. Gigmes, J. P. Fouassier, J. Lalevée, Design of new Type I and Type II photoinitiators possessing highly coupled pyrene–ketone moieties, Polymer Chemistry, 2013, 4.7, 2313-2324.

[16] C. Dietlin, S. Schweizer, P. Xiao, J. Zhang, F. Morlet-Savary, B. Graff, J. P Fouassier, J. Lalevée, Photopolymerization upon LEDs: new photoinitiating systems and strategies, Polymer Chemistry, 2015, 6.21, 3895-3912.

[17] A. AL Mousawi, F. Dumur, P. Garra, J. Toufaily, T. Hamieh, F. Goubard, T.T. Bui, B. Graff, D. Gigmes, J.P. Fouassier, J. Lalevée, Azahelicenes as Visible Light Photoinitiators for Cationic and Radical Polymerization: Preparation of Photoluminescent Polymers and Use in High Performance LED Projector 3D Printing Resins, Journal of Polymer Science, 2017, Part A, 55, 1189–1199.

[18] J. Yu, Y. Gao, S. Jiang, F.Sun, Naphthalimide aryl sulfide derivative norrish type I photoinitiators with excellent stability to sunlight under near-UV LED, Macromolecules, 52.4, 1707-1717.

[19] F. Hammoud, N. Giacoletto, G. Noirbent, B. Graff, A. Hijazi, M. Nechab, D. Gigmes, F. Dumur, J. Lalevée, Substituent Effects on Photoinitiation Ability of

Coumarin-Based Oxime-Ester Photoinitiators for Free Radical Photopolymerization, Materials Chemistry Frontiers, 2021.

[20] Z.H. Lee, F. Hammoud, A. Hijazi, B. Graff, J. Lalevée, Y.C. Chen, Synthesis and free radical photopolymerization of triphenylamine-based oxime ester photoinitiators, Polymer Chemistry, 2021, 12, 1286-1297.

[21] W. Wang, M. Jin, H. Pan, D. Wan, Remote Effect of Substituents on the Properties of Phenyl Thienyl Thioether-based Oxime Esters as LED-sensitive Photoinitiators, Dyes and Pigments, 2021, 109435.

[22] M. Popal, J. Volk, G. Leyhausen, W. Geurtsen, Cytotoxic and genotoxic potential of the type I photoinitiators BAPO and TPO on human oral keratinocytes and V79 fibroblasts, Dental Materials, 2018, 34.12, 1783-1796.

[23] X. Peng, D. Zhu, P. Xiao, Naphthoquinone derivatives: Naturally derived molecules as blue-light-sensitive photoinitiators of photopolymerization, European Polymer Journal, 2020, 127, 109569.

[24] R. Strzelczyk, R. Podsiadły, Derivatives of 1, 4-naphthoquinone as visible-light-absorbing one-component photoinitiators for radical polymerisation. Coloration Technology, 2015, 131.3, 229-235.

[25] M. M. Abdul-Monem, Naturally Derived Photoinitiators for Dental and Biomaterials Applications, European Dental Research and Biomaterials Journal, 2020, 1.02, 72-78.

[26] F. Hammoud, Z.H. Lee, B. Graff, A. Hijazi, J. Lalevée, Y.C. Chen, Novel phenylamine-based oxime ester photoinitiators for LED-induced free radical, cationic, and hybrid polymerization, Journal of Polymer Science, 2021, 59, 1711–1723.

[27] M. Abdallah, D. Magaldi, A. Hijazi, B. Graff, F. Dumur, J.P. Fouassier, T.T. Bui, F. Goubard, J. Lalevée, Development of New High-Performance Visible Light Photoinitiators Based on Carbazole Scaffold and Their Applications in 3D Printing and Photocomposite Synthesis, J. Polym. Sci., Part A, 2019, 57, 2081–2092.

[28] L. M. Gornostaev, M. V. Vigant, O. I. Kargina, A. S. Kuznetsova, Y. G. Khalyavina, T. I. Lavrikova, Synthesis of 2-aryl-1-hydroxy-1H-naphtho [2, 3-d]

imidazole-4, 9-diones by reaction of 2-benzylamino-1, 4-naphthoquinones with nitric acid. Russian Journal of Organic Chemistry, 2013, 49.9, 1354-1357.

[29] K. A. Rykaczewski, E. R. Wearing, D. E. Blackmun, C. S. Schindler, Reactivity of oximes for diverse methodologies and synthetic applications, Nature Synthesis, 2022, 1.1, 24-36.

[30] J. R. Lakowicz, J. R. (Ed.), Principles of fluorescence spectroscopy. Boston, MA: springer US, 2006.

TOC graphic:

Naphthoquinone-based Imidazolyl Esters as Blue-Light-Sensitive Type I and Type II Photoinitiators